Scientia Iranica D (2018) 25(3), 1571–1581

Sharif University of Technology
Scientia Iranica
*Transactions D: Computer Science & Engineering and Electrical Engineering*
http://scientiairanica.sharif.edu

# Optimization of radiation characteristic of time modulated circular geometry using DEWM

**G. Ram[a,*], D. Mandal[b], S.P. Ghoshal[b], and R. Kar[b]**

a. *Department of ECE, Madanpalle Institute of Technology and Science, India.*
b. *Department of Electrical Engineering, National Institute of Technology Durgapur, India.*

Received 20 January 2016; received in revised form 21 October 2016; accepted 29 May 2017

**KEYWORDS**
Side Lobe Level (SLL);
TMHSCAA;
TMCCAA;
RF switch;
DEWM;
First null beamwidth (FNBW).

**Abstract.** In this paper, Differential Evolution with Wavelet Mutation (DEWM) is applied to the radiation pattern synthesis of circular geometries of antenna array. Two circular geometries have been considered: (a) Time-Modulated Half-Symmetric Circular Antenna Array (TMHSCAA); (b) 9-ring Time Modulated Concentric Circular Antenna Array (TMCCAA). DEWM algorithm is applied to show the performance improvement of the optimal designs of TMHSCAA and TMCCAA. While doing so, various other stochastic algorithms, such as Real coded Genetic Algorithm (RGA), Particle Swarm Optimization (PSO), and Differential Evolution (DE), are used for the sake of comparison to establish the superiority of DEWM. For TMHSCAA, elements are symmetrical around the vertical axis; therefore, the number of parameters to be optimized is reduced with two control parameters, such as switching excitation phase of each element. For TMCCAA, two proportional case studies, Case 1 and Case 2, are investigated with different variable parameters. The simulation outcomes show the supremacy of DEWM to be a plausible claimant for scheming the best TMHSCAA and TMCCAA. The simulation tests have also been performed with 20- and 36-element TMHSCAAs and 9-ring TMCCAA.



## 1. Introduction

Circular antenna array is the congregation of a similar type of elements in a circular fashion. The radiation pattern obtained by the antenna array is controlled by various parameters [1-2]. Previous research works have shown that the time modulated linear antenna arrays are attractive for the synthesis of low/ultralow sidelobes [3-11]. The conventional antenna array can be considered as the radiation source distributed in space, usually of three dimensions [1-2].

In [3-5], time-modulation technique is used to carry out a preferred radiation patterns by exploiting the on-off switching of the array elements. This feature can help to accomplish a better radiation pattern than those of the traditional antenna array synthesis methods. Usually, the radiation source of an antenna has three dimensions. Consequently, the flexibility to control the radiation pattern is restricted; alternatively, the installation cost is excessively high. The time modulation concept extensively employed in the antenna array achieves the low side lobe radiation characteristics even with the uniform current excitation weights. The same concept of time modulation has also been extended into circular arrays. The fundamental problem associated with the time-modulated array is

*. *Corresponding author.*
*E-mail addresses: gopi203hardel@gmail.com (G. Ram); durbadal.bittu@gmail.com (D. Mandal); spghoshalnitdgp@gmail.com (S.P. Ghoshal); rajibkarece@gmail.com (R. Kar)*

doi: 10.24200/sci.2017.4372

that they generate harmonics, or sidebands at the multiples of the switching frequency [6-9]. A number of researches on Time Modulated Antenna Arrays (TMAAs) have followed this work. Yang et al. carried out a series of studies on 4D antenna arrays including various features mentioned in [6,7,9-12].

The key feature of a circular ring array is the cylindrical symmetry of its radiation pattern and of compact structure, thus finding considerable interest in various applications including radio direction finding [1], radar [13], communication [14], and electronic countermeasures, navigation and imaging [15].

Different evolutionary algorithms, such as Genetic Algorithm (GA) [16-18], Particle Swarm Optimization (PSO) [19-22], and Differential Evolution (DE) [6], [20-21], have been employed for low sidelobe array pattern synthesis of Concentric Circular Antenna Arrays (CCAA) [22-34]. The application of evolutionary algorithms has spread to many fields of engineering, including electromagnetics [35-42]. In this work, two different geometries of circular array are studied:

a) For sidelobe reduction and less complexity, the TMHSCAA is applied;

b) For simultaneous reduction of sidelobe and improvement in directivity, the uniformly excited Time-Modulated Concentric Circular Antenna Array (TMCCAA) [20-21] is applied.

For optimization of TMCCAA and TMHSCAA's variables, DEWM is applied [42], while keeping the current amplitude excitations uniform.

The remaining part of the paper is divided as follows. In Section 2, the theoretical analyses of TMHSCAA and TMCCAA are presented. Section 3 briefly explains the proposed DEWM-based approach to the designs of TMHSCAA and TMCCAA. Section 4 describes the simulation results with the proposed DEWM-based approach. Section 5 shows the convergence figures of the adopted algorithm. Finally, Section 6 concludes the paper.

## 2. Theoretical analysis

### *2.1. Time Modulated Half Symmetric Circular Antenna Array (TMHSCAA)*

Consider a time-modulated circular array of $M$ $(= 4N)$ isotropic elements, equally spaced on the $x - y$ plane shown in Figure 1(a). Each array element can be turned ON or OFF by RF switch. The circular array is symmetric with respect to the $y$-axis. The array is excited by a uniform amplitude excitation, $I_n = I$; the phase and switching time of $n$ elements are $\alpha_n$ and $\tau_n$, respectively, for $n = (-N+1)...0, 1, 2...(N-1)$, where $n$ is the index of the array elements. $\alpha_N$ and $\alpha_{-N}$ are the asymmetric phases of elements $N$ and $-N$, respectively. Similarly, the switching time sequences of elements are $\tau_n$ for $n = (-N+1)...0, 1, 2...(N-1)$. $\tau_N$ and $\tau_{-N}$ are switching time sequences of elements $N$ and $-N$, respectively.

The number of elements in the circular array in Figure 1(a) is symmetrical with respect to $y$-axis. The elements in the array are not symmetric along the $x$-axis. In the same figure, dotted line shows the pair of symmetrical elements $[n = (-N+1)...0, 1, 2...(N-1)]$ along the $y$-axis. Therefore, due to symmetrical elements, the number of elements participating in the optimization is $M/2(-N$ to $N)$. $\alpha_{-n}$ and $\alpha_n$ are not interrelated because array is not symmetric in the $x$-axis and is used as the optimizing parameter of the evolutionary algorithms. Similar explanation is applicable to $\tau_n$ and $\tau_{-n}$.

However, in the conventional uniform antenna array (not optimizing using evolutionary algorithms), there may be a progressive excitation phase relation between the elements $(\alpha_n = -\alpha_{-n})$ with uniform switching time sequence $(\tau_n = \tau_{-n})$.

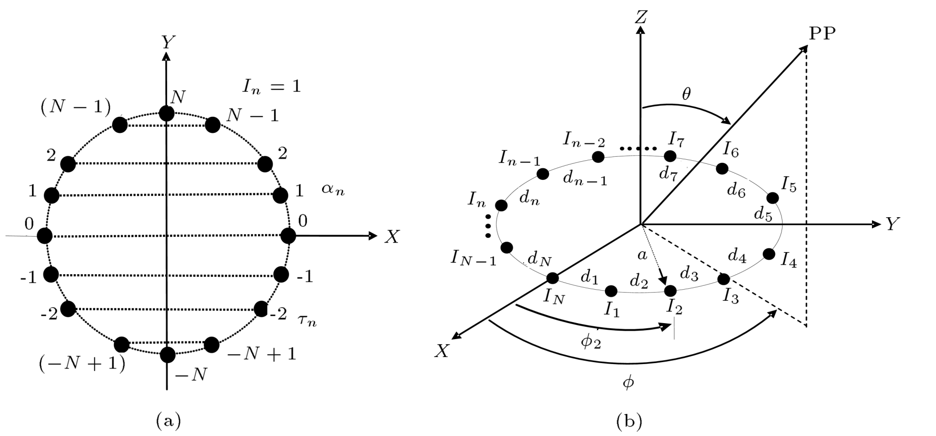


**Figure 1.** (a) Circular array of 4N elements. (b) Geometry of a circular array laid on the $x - y$ plane with $N$ isotropic elements scanning at a point PP in the far field.

Now, the Array Factor (AF) of this array in the azimuth plane ($\theta = 90°$) can be written as follows [21]:

$$AF(\phi,t) = \gamma e^{j2\pi f_0 t} \sum_{n=-N}^{N} I_n U_n(t) \cos \left[ka\cos(\phi + \frac{2n\pi}{M}) + \alpha_n\right], \quad (1)$$

where:

$$\gamma = \begin{cases} 2 & \text{for } n = -N+1, .... \\ & -2......0.....2....N+1 \\ 1 & \text{for } n = \{-N, N\} \end{cases} \quad (2)$$

After applying the time modulation concept, each element of the circular array is controlled by a high-speed periodic Radio Frequency (RF) switch $U_n(t)$ [6], with periodic switch-on time sequence function as given by:

$$U_n(t) = \begin{cases} 1 & \text{for } 0 \le t \le \tau_n \\ 0 & \text{otherwise} \end{cases} \quad (3)$$

From Eqs. (1) to (3), it can be written as follows:

$$AF(\phi,t) = \sum_{m=-\infty}^{\infty} \sum_{n=-N}^{N} \gamma e^{j2\pi(f_0+m.F_p)t} i_{mn} \cos\left[ka\cos(\phi + \frac{2n\pi}{M}) + \alpha_n\right], \quad (4)$$

where:

$$i_{mn} = \frac{I_n \tau_n}{T_p} \sin c(\pi m F_p \tau_n) e^{-j\pi m F_p \tau_n}. \quad (5)$$

Due to the periodicity of $U_n(t)$, array factor (1) can be decomposed into a Fourier series which has different harmonic frequency components $f_0 + m.F_p(m = 0, \pm1, \pm2, ..., \pm\infty)$. Therefore, sideband components $(f_0 + m.F_p, m \neq 0)$ have radiation patterns, which can be formulated as follows:

$$AF_m(\phi,t) = \gamma e^{j2\pi(f_0+m.F_p)t} \sum_{n=-N}^{N} i_{mn} \cos\left[ka\cos(\phi + \frac{2n\pi}{M}) + \alpha_n\right]. \quad (6)$$

The amplitudes of the Fourier components can be written as $i_{0n} = I_n.\tau_n/T_p$ at the centre frequency $(m = 0)$. The far field of Eq. (6) contains the $m$th harmonic frequency components, $m.F_p$, where $(m = 0, \pm1, \pm2, ..., \pm\infty)$. From Eq. (6), one can express array factors $AF_0(\theta,\phi,f)$, $AF_1(\theta,\phi,f)$, and $AF_2(\theta,\phi,f)$ for the operating frequency, the first positive sideband, and the second positive sideband, respectively.

The next task in the optimization process is to define the objective function. Objective function is the function that is used to optimize the variable parameters of the Array Factor (AF) of an antenna array. Since the main aim of the objective function in this paper is to reduce the Side Lobe Level (SLL), this problem is termed as the minimization problem. To design a proper and an effective objective function, two different control parameters (switching time sequence and the excitation phase of the elements) have been considered for the optimal synthesis radiation pattern TMHSCAA. The excitation amplitude of each ring is made uniform being equal to 1. This assumption of unity amplitude has been made due to high Dynamic Range Ratio (DRR) of the optimal current excitation weights, which is very difficult to implement practically in the feed network. Dynamic Range Ratio (DRR) is the ratio of the maximum to the minimum normalized optimal current excitation weights of the array. The Objective Function (OF) of improving the SLL of radiation pattern for TMHSCAA is given in Eq. (7):

$$\begin{aligned} OF = & w_1 \times |AF_0(\phi_1,t) + AF_0(\phi_2,t)| \,/\, |AF_0(\phi_{0c},t)| \\ & + w_2 \times \frac{1}{(\phi_1+\pi)} \int_{-\pi}^{\phi_1} AF_0(\phi,t)\, d\phi \\ & + \frac{1}{(\pi-\phi_2)} \int_{\phi_2}^{\pi} AF_0(\phi,t)\, d\phi \\ & + w_3 \times [FNBW_{\text{computed}} - FNBW(I_n = 1)] \\ & + w_4 \times |\phi_{0c} - \phi_{0i}|. \end{aligned} \quad (7)$$

Eq. (7) represents the minimization problem of the objective function. Herein, $\phi_{0c}$ is the angle where the highest peak of main beam of the computed radiation pattern of TMHSCAA is attained in $\phi \in [-\pi,\pi]$ at the current iteration cycle with the adopted evolutionary algorithms. $\phi_{0i}$ is the angle where the maximum peak of the initial radiation pattern (without optimization) of $AF_0(\phi,t)$ takes place. $\phi_1$ and $\phi_2$ are the locations of the first nulls at the left and right parts of the main beam computed radiation pattern. The first term is used to reduce either sides of the SLL of the radiation pattern having the SLL in the range of $\phi \in [-\pi,\phi_1]$ and $\phi \in [\phi_2,\pi]$. The second term is used to minimize the area covered by the SLL of the radiation pattern of the array. The third term is used to maintain $FNBW_{\text{computed}}$ of computed radiation pattern with respect to $FNBW(I_n = 1)$. $w_1$, $w_2$, $w_3$ and $w_4$ are the weighting factors chosen as 18, 18, 12, and

12, respectively, so that the first and second terms dominate to some extent over those of the third and fourth terms.

### 2.2. Design of Time-Modulated Concentric Circular Antenna Array (TMCCAA)

Let us consider CCAA with $P$ concentric circular rings, where the $p$th ($p = 1, 2, ..., P$) ring has a radius $r_p$ and the corresponding number of elements in each ring is $N_p$ as shown in Figure 2. From Figure 2, the array factor for TMCCAA, AF$(\theta, t)$, can be written [20] as follows:

$$AF(\theta, t) = e^{j2\pi f_0 t}\left\{1 + \sum_{p=1}^{P}\sum_{i=1}^{N_p} I_p U_p(t) \exp[jkr_p \sin\theta\cos(\phi - \phi_{pi})]\right\}, \quad (8)$$

where $I_p$ is the excitation amplitude of an element on the $p$th circular ring (where $I_p = 1$ throughout this study); $k = 2\pi/\lambda$; $\lambda$ is the wave-length of the signal. $\theta$ and $\phi$ are elevation and azimuth angles, respectively. In this paper, $\phi = 0°$ is considered. Angle $\phi_{pi}$ is the element-to-element angular separation measured from the positive $x$-axis. Operating frequency is $f_0$ in (Hz). $T_0$ is the time period of the operating frequency. Each element is turned 'ON' for the fixed time duration of $\tau_p(0 \leq \tau_p \leq T_{prf})$ with a pulse repetition frequency of $f_{prf} = 1/T_{prf}$ where $T_{prf}(\tau_p \leq T_{prf} > T_0)$ is the pulse repetition period:

$$\phi_{pi} = 2\pi\left(\frac{i-1}{N_p}\right) \quad p = 1, ..., P; \quad i = 1, ..., N_p. \quad (9)$$

There are nine rings where radius of the each ring is given by $r_p = p\lambda/2$, where $p = 1, ..., P$ and $d_p$ is the uniform inter-element spacing between the elements in the ring. Then, the number of elements in the $p$th ring $p$th is given by [29]:

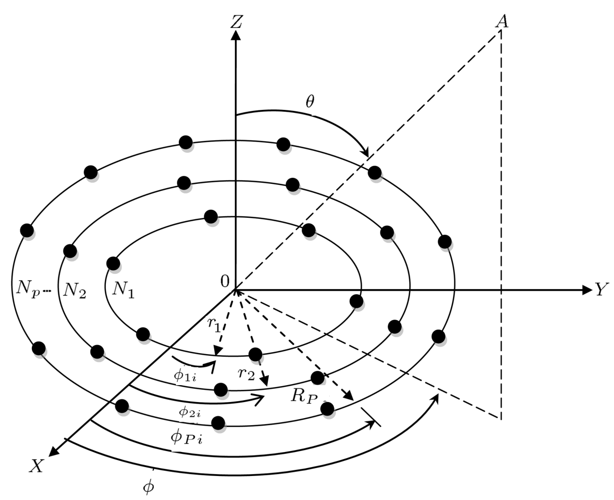


**Figure 2.** Concentric Circular Antenna Array (CCAA).

$$N_p = \frac{2\pi r_p}{d_p} = 2\pi p. \quad (10)$$

Since the number of elements must be an integer, the value in Eq. (10) must be rounded up or down. To keep $d_p \geq \lambda/2$ and allow sufficient element spacing, the digits to the right of the decimal point are dropped.

$\phi_p$ is not just $\phi_p$, it is represented as $\phi_{pi}$ given in Eq. (11) which is the azimuthal angle from the $x$-axis to the $i$th element of the $p$th ring:

$$\phi_{pi} = 2\pi\left(\frac{i-1}{N_p}\right) \quad p = 1, ..., P; \quad i = 1, ..., N_p, \quad (11)$$

$d_p$ is the uniform inter-element spacing of each element in the $p$th ring. In this paper, the optimized value of the inter-element spacing ($d_p$) is uniform for the entire ring. This is the reason why the optimized inter-element spacing achieved by the adopted algorithm is uniform for all the rings, as shown in the Table 3 in the result Section.

Periodic switch ON-OFF function $U_p(t)$ [6] in time domain representation can be decomposed into Fourier series in frequency domain, as given by the following:

$$U_p(t) = \sum_{m=-\infty}^{\infty} a_{mp} e^{j2\pi m f_{prf} t}, \quad (12)$$

where:

$$a_{mp} = \frac{I_p \tau_p}{T_{prf}} \sin c(m f_{prf} \tau_p) e^{-j\pi m f_{prf} \tau_p}. \quad (13)$$

Eq. (13) shows the current excitation values of the $m$th RF switch modulation frequency; $m = 0$ is used for the operating frequency. By substituting the value of $a_{mp}$ from Eq. (13) into Eq. (12) and from Eq. (12) into Eq. (8), Eq. (8) can be written as follows:

$$AF_m(\theta, t) = e^{j2\pi(f_0 + m.f_{prf})t}\left\{1 + \sum_{p=1}^{P}\sum_{i=1}^{N_p} a_{mp} \exp[jkr_p \sin\theta\cos(\phi - \phi_{pi})]\right\}. \quad (14)$$

The far field of Eq. (14) contains the $m$th harmonic frequency components $m.f_{prf}$, where $p = 0, \pm 1, \pm 2, ..., \pm\infty$. From Eq. (14), the array factors for the operating frequency, the first positive sideband, and the second positive sideband can be obtained. The directivity, $P_0$, at the fundamental (centre) frequency, $P_{(SR)}$ at the harmonic frequency, and dynamic efficiency are given as follows.

The power radiated by TMCCAA, $P_0$, at the fundamental (centre) frequency is given by Eq. (15) [20]:

$$P_0 = \int_0^{2\pi}\int_0^{\pi} |AF_0(\theta, \phi)|^2 \sin\theta d\theta d\phi. \quad (15)$$

The power radiated by TMCCAA, $P_{SR}$, at the harmonic frequency is given by Eq. (16) [20]:

$$P_{SR} = \sum_{\substack{m=-\infty,\\ m\neq 0}}^{\infty} \int_0^{2\pi}\int_0^{\pi} |AF_m(\theta,\phi)|^2 \sin\theta d\theta d\phi. \quad (16)$$

Thus, from Eq. (16), powers radiated at the first harmonic frequency ($P_1$) and second harmonic frequency ($P_2$) are given by Eqs. (17) and (18), respectively:

$$P_1 = \int_0^{2\pi}\int_0^{\pi} |AF_1(\theta,\phi)|^2 \sin\theta d\theta d\phi, \quad (17)$$

$$P_2 = \int_0^{2\pi}\int_0^{\pi} |AF_2(\theta,\phi)|^2 \sin\theta d\theta d\phi. \quad (18)$$

Dynamic efficiency ($\eta_d$) is defined as the ratio of power radiated by the array at the centre frequency and the sum of powers radiated by the array at the fundamental (centre) frequency as well as at the harmonic frequencies, and it is given by Eq. (19) [20]:

$$\eta_d = \frac{1}{1+\frac{\sum\limits_{\substack{m=-\infty,\\ m\neq 0}}^{\infty}\int_0^{2\pi}\int_0^{\pi}|AF_m(\theta,\phi)|^2\sin\theta d\theta d\phi}{\int_0^{2\pi}\int_0^{\pi}|AF_0(\theta,\phi)|^2\sin\theta d\theta d\phi}}. \quad (19)$$

The objective function is expressed as follows:

$$\begin{aligned} f^g_{\text{fitness}}(\tau_P, r_p, d_p) &= w_{11} * SLL^g_{\max}(\tau_P, r_p, d_p)|_{f_0} \\ &+ w_{22} * SBL^g_{\max}(\tau_P, r_p, d_p)|_{f_0+f_{prf}} \\ &+ w_{33} * SBL^g_{\max}(\tau_P, r_p, d_p)|_{f_0+2f_{prf}} \\ &+ w_{44} * (1/D_{TMCCA\_\max}), \end{aligned} \quad (20)$$

where $g$ denotes the $g$th iteration cycle, $SLL_{\max}|_{f_0}$ is the maximum $SLL$ at the centre frequency, $SBL_{\max}|_{f_0+f_{prf}}$ is the maximum sideband level ($SBL$) at the first sideband frequency, and $SBL_{\max}|_{f_0+2f_{prf}}$ is the maximum sideband level ($SBL$) at the second sideband frequency. $w_{11}$, $w_{22}$, $w_{33}$, and $w_{44}$ are the weighting factors where each term is used to emphasize different contributions to the fitness function. $D_{\text{TMCCA}-\max}$ is the maximum directivity of the TMCCAA.

## 3. Numerical results

### *3.1. Time Modulated Half Symmetric Circular Antenna Array (TMHSCAA)*

The control parameters of RGA, PSO, DE, and DEWM are given in [20]; therefore, these are not mentioned in this paper. The MATALB simulation results are obtained for TMHSCAA with 20 and 36 elements, respectively, to show the usefulness of the SLL reduction. RGA, PSO, DE, and DEWM algorithms are individually employed to explore the range of excitation phase, $\alpha_n$, with $[-\pi,\pi]$ (in radians). The normalized switch-on time intervals ($\tau_n/T_{prf}$) are explored within [0.06, 1.0].

In this paper, two kinds of comparisons are performed. The first comparison is to show the superiority of the adopted algorithm over the other algorithms. On the other hand, two different geometric conditions of TMHSCAA are considered. In the case of time-modulated half-symmetric circular arrays (TMHSCAA), inter-element spacing is kept as $\lambda/4$ ($ka = M/4$) with uniform amplitude excitation and inter-element spacing where $M$ is the number of elements in the array. Due to the symmetry of the array of 20- and 36-element arrays, only 11 and 19 variables of switching time sequences and excitation phases of elements together need to be optimized by RGA, PSO, DE, and DEWM algorithms. Figures 3 and 4 show the optimal radiation patterns obtained by different algorithms for 20- and 36-element TMHSCAAs, respectively. The figures also illustrate the normalized radiation patterns at $f_0$ as well as at the first two sideband frequencies $f_0 + F_p$ and $f_0 + 2F_p$. Table 1 shows the switching time sequence and the phase excitation of each element obtained for 20- and 36-element arrays by DEWM for

**Table 1.** Switching time sequence and phase excitation of each element obtained by DEWM for TMHSCAA.

| No. of elements | Switching time sequence of each element | Phase excitation of each elements (in radian) |
|---|---|---|
| 20 | 0.6123 0.0932 0.0748 0.0822<br>0.2389 0.1205 0.2891 0.1410<br>0.2283 0.2596 0.3571 | 0.0073 -5.1906 -1.0452 2.1162 -3.2233<br>3.0408 2.6799 10.7148 1.5282 -1.4367<br>1.5863 |
| 36 | 0.7639 0 0.3926 0.2868<br>0.1792 0.2910 0.1085 0.6367<br>0.5688 0.5930 0.4682 0.4295<br>0.4234 0.2444 0.5350 0.7760<br>0.1673 0.4971 0.2912 | -1.7052 1.7820 -1.1310 -1.5917 1.2706<br>-5.0370 7.6393 1.0489 -1.2165 0.7732<br>-0.9896 1.0105 -17.2823 -0.3700<br>2.0089 -1.1275 2.6634 5.0737 41.5982 |

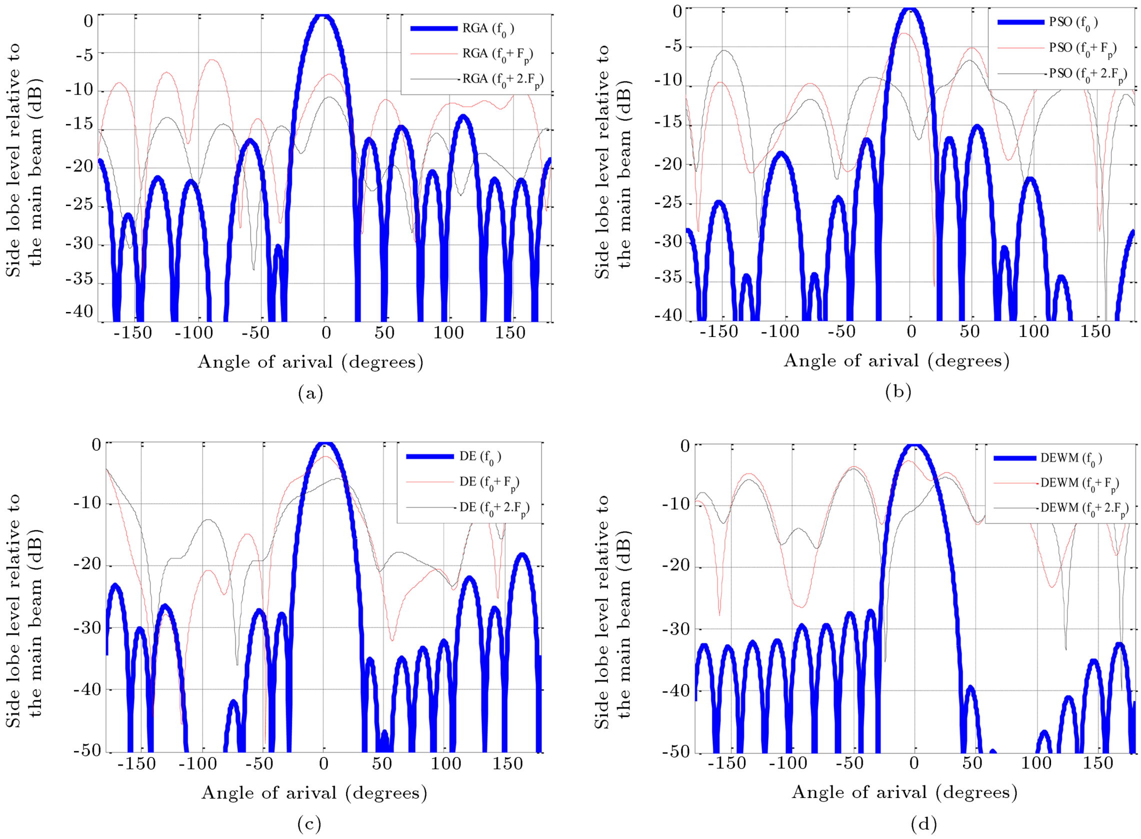


**Figure 3.** Optimal radiation patterns obtained by different algorithms for 20-element TMHSCAA.

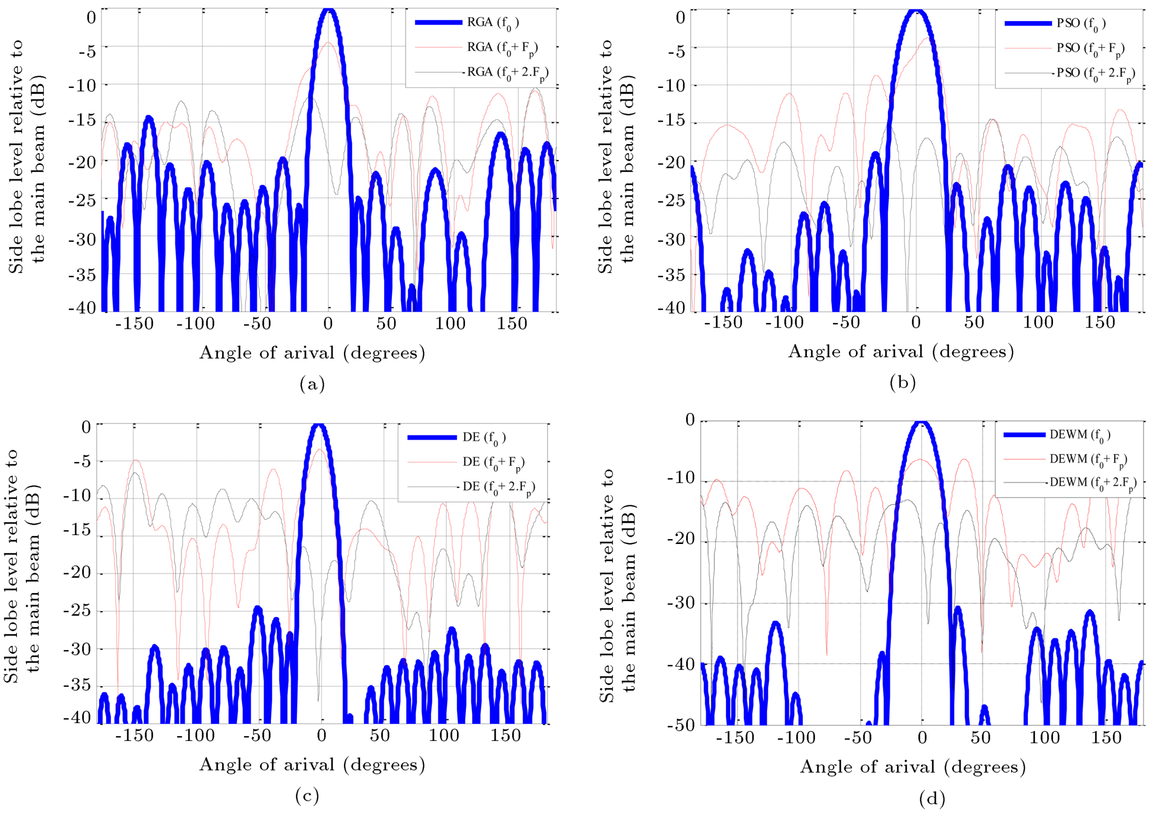


**Figure 4.** Optimal radiation patterns obtained by different algorithms for 36-element TMHSCAA.

**Table 2.** SLL and FNBW obtained by various algorithms for TMHSCAA for 20 and 36 elements.

| Algorithm | TMHSCAA No. of elements 20 SLL (dB) | TMHSCAA No. of elements 20 FNBW (deg.) | TMHSCAA No. of elements 36 SLL (dB) | TMHSCAA No. of elements 36 FNBW (deg.) |
|---|---|---|---|---|
| RGA | -13.39 | 58.3200 | -14.48 | 38.8800 |
| PSO | -15.25 | 48.9600 | -19.09 | 51.8400 |
| DE | -18.29 | 62.2800 | -24.62 | 41.4000 |
| DEWM | -27.02 | 69.8400 | -30.93 | 53.2800 |

**Table 3.** The optimal values of optimized parameters of Case 1, and Case 2 obtained by DEWM for TMCCAA.

| Case studies | Optimization parameters | Ring no. 1 | 2 | 3 | 4 | 5 | 6 | 7 | 8 | 9 |
|---|---|---|---|---|---|---|---|---|---|---|
| Case 1 | $\tau_p$ ($\mu s$) | 0.7685 | 0.9956 | 0.8964 | 0.6980 | 0.5201 | 0.4407 | 0.5268 | 0.4089 | 0.2578 |
| Case 2 | $\tau_p$ ($\mu s$) | 0.8323 | 0.8638 | 0.7610 | 0.6664 | 0.5140 | 0.3826 | 0.2700 | 0.1725 | 0.0953 |
| | $\gamma_p$ ($\lambda$) | 0.7479 | 1.5894 | 2.4290 | 3.2952 | 4.1564 | 5.0188 | 5.8988 | 6.7657 | 7.5556 |
| | $d_p$ ($\lambda$) | 0.8469 | 0.8469 | 0.8469 | 0.8469 | 0.8469 | 0.8469 | 0.8469 | 0.8469 | 0.8469 |
| | $N_r$ | 5 | 11 | 18 | 24 | 30 | 37 | 43 | 50 | 56 |

TMHSCAA. Table 2 shows the SLL and FNBW values obtained by various algorithms for TMHSCAA of 20- and 36-element arrays. From the simulation results and Table 2, it is clear that the SLL obtained by DEWM algorithm is the lowest among those obtained by RGA, PSO, and DE for both cases of 20- and 36-element arrays. The SLL results obtained by the TMHSCAA for 20 and 36 elements are much superior to the SLL results obtained by the conventional circular arrays with the same number of elements, respectively. The reasons for the outperformance of TMHSCAA are due to: (a) the symmetric arrangement of elements in TMHSCAA, (b) half reduction of the number of optimizing switching times and excitation phases of the elements, and (c) less computation complexity of the algorithm.

### *3.2. Time-Modulated Concentric Circular Antenna Array (TMCCAA)*

This section shows the MATLAB simulation results of TMCCAA designs obtained by DEWM. Let us consider $c$ as the speed of light, $f_0$ as the operating frequency, $f_{prf} = 1/T_{prf}$ as time modulation frequency, where $T_{prf}$ is the pulse repetition time. Uniformly excited conventional CCAA is having SLL of -17.4 dB, FNBW of 14.76 degrees, and directivity of 29.35 dB.

- ***Case 1. Optimization of only switching time instant of each ring:*** In this case study, only switching time instant is optimized using DEWM; however, all the radiation pattern control parameters are kept unaltered as the uniform CCAA. Table 3 shows the optimal values of optimized parameters of Case 1 and Case 2 obtained by DEWM for TMCCAA. From Table 4, for Case 1, DEWM outperforms PSO [20], DE [20], uniform CCAA, and the reported result in [22].
- ***Case 2. Optimized switching time instant, ring radii and optimal uniform inter-element spacing:*** In this case study, switching time instant, ring radii, and optimal uniform inter-element spacing are optimized using DEWM. From Table 4, for Case 2, DEWM outperforms PSO [20], DE [20], uniform CCAA, and the result reported in [20,22,29]. Figures 5 and 6 show the radiation patterns (dB) obtained by DEWM for Cases 1 and Case 2, respectively.

## 4. Convergence profile of DEWM

This section shows the comparative performance analysis of the algorithm. The convergence curve is plotted for the fitness function against the iteration cycle.

**Table 4.** Optimal SLL, SBL1, SBL2, FNBW, P0, P1, P2, directivity, and dynamic efficiencies of TMCCAA obtained by DEWM.

| | Case | SLL (dB) | SBL1 (dB) | SBL2 (dB) | FNBW (deg.) | $P_0$ (W) | $P_1$ (W) | $P_2$ (W) | Directivity (dB) | Dynamic efficiency |
|---|---|---|---|---|---|---|---|---|---|---|
| DEWM | Case 1 | -26.04 | -6.604 | -17.79 | 18.3600 | 656.56 99 | 182.4114 | 41.3873 | 27.5467 | 74.5790 |
| | Case 2 | -38.53 | -6.835 | -11.55 | 13.6800 | 173.1415 | 59.8461 | 39.2741 | 29.6092 | 63.5938 |
| DE [20] | Case 1 | -24.78 | -5.782 | -14.21 | 16.2000 | 605.2354 | 195.5965 | 45.4418 | 26.8062 | 71.5177 |
| | Case 2 | -31.83 | -5.737 | -12.73 | 14.7600 | 301.5714 | 117.6263 | 35.6558 | 28.9594 | 66.3008 |
| PSO [20] | Case 1 | -24.6 | -6.586 | -15.54 | 16.5600 | 707.8121 | 198.4451 | 42.1154 | 26.6365 | 74.6344 |
| | Case 2 | -30.98 | -7.481 | -13.09 | 15.1200 | 273.8105 | 86.6163 | 37.5827 | 28.6277 | 68.7950 |

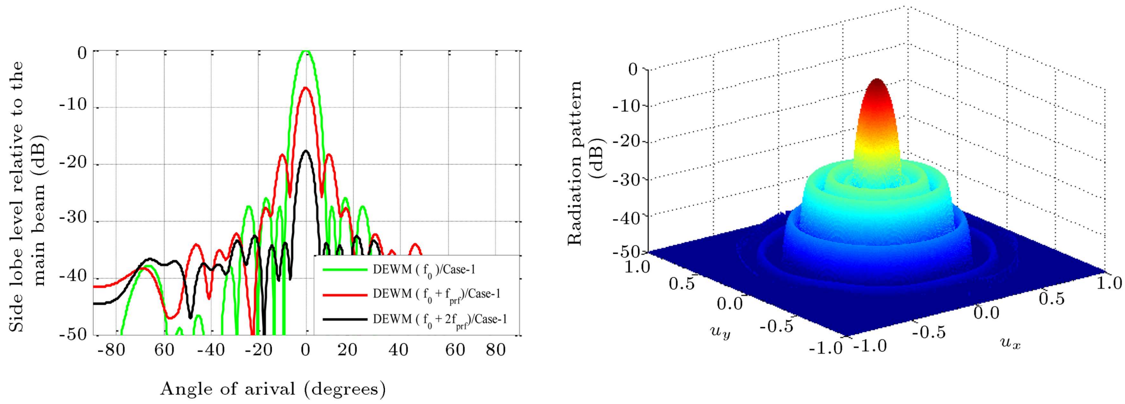


(a) (b)

**Figure 5.** Radiation patterns obtained for Case 1 by DEWM: (a) 2D pattern and (b) 3D pattern.

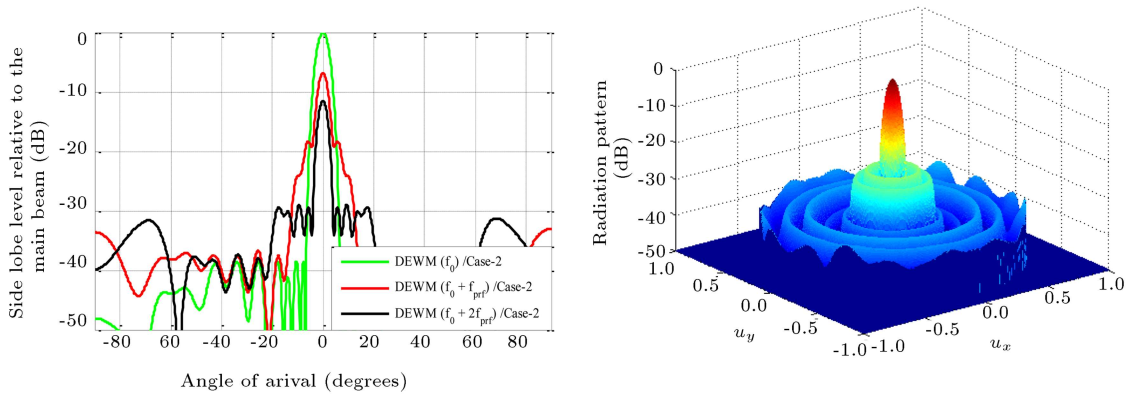


(a) (b)

**Figure 6.** Radiation patterns obtained for Case 2 by DEWM: (a) 2D pattern and (b) 3D pattern.

From Figure 7, it is clear that DEWM gives a better convergence performance over PSO [20], and DE [20]. The programming was written in MATLAB language using MATLAB 7.5 on dual core (TM) processor, 2.88 GHz with 1 GB RAM.

## 5. Conclusion

This paper deals with two different types of time-modulated circular antenna array geometries. The uniform current excitation and equal inter-element spacing based Time-Modulated Half-Symmetric Circular Antenna Array (TMHSCAA) are designed, which efficiently synthesize much lower SLLs as compared with those of the conventional arrays in the azimuthal plane. In the single ring TMCCAA, the elements have been designed so that it is symmetric in the vertical axis; thus, it has become the Time-Modulated Half-Symmetrical Circular Antenna Array (TMHSCAA). The Differential Evolution with Wavelet Mutation (DEWM) is applied as an efficient algorithm to optimize the excitation phase and the switch-on time

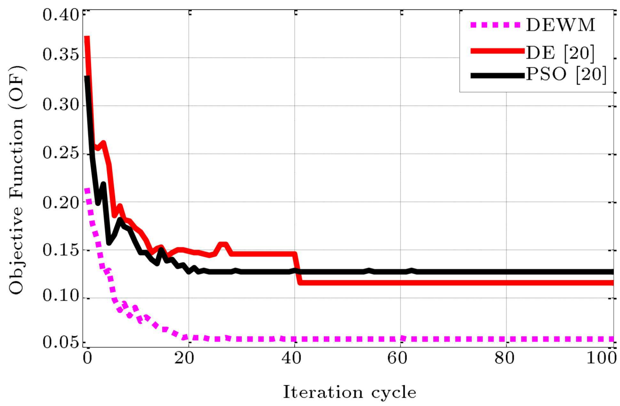


**Figure 7.** Convergence profile obtained by DEWM for Case 2 of TMCCAA.

interval of each element of TMHSCAA and TMCCAA. For 9-ring, 279-element TMCCAA with respect to sidelobe level, first-null beamwidth, and directivity, the performance of the DEWM proves to be better than PSO and DE. In TMCCAA, Case 2 outperforms Case 1 and the uniform concentric circular antenna array with respect to SLL, FNBW, and directivity. Numerical results show that the results obtained by DEWM algorithm are much better than those of [20,22,29]. For TMHSCAA, of 20- and 36-element arrays, DEWM obtains the lowest SLL patterns over those of the conventional array and other algorithms such as RGA, PSO and DE. The study presented here shows that the TMHSCAA is a promising array that can be used to synthesize much lower sidelobe patterns and also can be easily extended to the synthesis of other preferred beams. The proposed method can be applicable to different geometrical configurations with time modulation techniques.

## References


1. Ballanis, A., *Antenna Theory Analysis and Design*, 2nd Ed., John Willey and Son's Inc., New York (1997).
2. Elliott, R.S., *Antenna Theory and Design*, Revised edition, John Wiley, New Jersey (2003).
3. Shanks, H.E. and Bickmore, R.W. "Four-dimensional electromagnetic radiators", *Canad. J. Phys.*, **37**, pp. 263-275 (Mar. 1959).
4. Kummer, W.H., Villeneuve, A.T., Fong, T.S., et al. "Ultra-low sidelobes from time-modulated arrays [J]", *IEEE Trans. Antennas Propagat.*, **11**(5), pp. 633-639 (1963).
5. Lewis, B.L. and Evins, J.B. "A new technique for reducing radar response to signals entering antenna sidelobes [J]", *IEEE Trans. Antennas Propagat.*, **31**(6), pp. 993-996 (1983).
6. Yang, S., Gan, Y.B., and Qing, A. "Sideband suppression in time modulated linear arrays by the differential evolution algorithm", *IEEE Antennas Wirel. Propag. Lett.*, **1**, pp. 173-175 (2002).
7. Yang, S., Gan, Y.B., and Tan, P.K. "A new technique for power-pattern synthesis in time-modulated linear arrays", *IEEE Antennas Wirel. Propag. Lett.*, **2**, pp. 285-287 (2003).
8. Fondevila, J., Bregains, J.C., Ares, F., and Moreno, E. "Optimizing uniformly excited arrays through time modulation", *IEEE Antennas Wirel. Propag. Lett.*, **3**, pp. 298-301 (2004).
9. Yang, S., Gan, Y.B., Qing, A., and Tan, P.K. "Design of a uniform amplitude time modulated linear array with optimized time sequences", *IEEE Trans. Antennas Propag.*, **53**(7), pp. 2337-2339 (2005).
10. Yang, S., Gan, Y.B., and Qing, A. "Antenna array pattern nulling using a differential evolution algorithm", *Int. J. RF Microwave Computer-Aided Eng.*, **14,** pp. 57-63 (January 2004).
11. Zhu, Q., Yang, S., and Zheng, L. "Design of a low sidelobe time modulated linear array with uniform amplitude and sub-sectional optimized time steps", *IEEE Transactions on Antennas and Propagation*, **60**(9), pp. 4436-4439 (2012).
12. Yang, S., Beng, Y., and Tan, P.K. "Evaluation of directivity and gain for time-modulated linear antenna arrays", *Microwave and Optical Technology Letters*, **42**(2), pp. 167-171 (July 2004).
13. Munson, D.C., Brian, J.D.O., and Jenkins, W.K. "A tomographic formulation of spot-light mode synthetic aperture radar", *Proc. IEEE*, **71**, pp. 917-925 (August 1983).
14. Compton, R.T. "An adaptive array in a spread-spectrum communication system", *Proc. IEEE*, **66**, pp. 289-298 (March 1978).
15. Kak, A.C., *Array Signal Processing*, S. Haykin, Ed., Prentice- Hall, Englewood Cliffs, NJ (1985).
16. Panduro, M.A., Mendez, A.L., Dominguez, R. and Romero, G. "Design of non-uniform circular antenna arrays for side lobe reduction using the method of genetic algorithms", *Int. 1. Electron. Commun. (AEU)*, **60**, pp. 713-717 (2006).
17. Rooeinfar, R., Azimi, P., and Pourvaziri, H. "Multi-echelon supply chain network modelling and optimization via simulation and metaheuristic algorithms", *Scientia Iranica*, **23**(1), pp. 330-347 (2016).
18. Panduro, M.A., Brizuela, C.A., Balderas, L.I., and Acosta, D.A. "A comparison of genetic algorithms, particle swarm optimization and the differential evolution method for the design of scannable circular antenna arrays", *Progress in Electromagnetics Research B*, **13**, pp. 171-186 (2009).
19. Shihab, M., Najjar, Y., Dib, N., and Khodier, M. "Design of non-uniform circular antenna arrays using particle swarm optimization", *Journal of Electrical Engineering*, **59**(4), pp. 216-220 (2008).
20. Ram, G., Mandal, D., Kar, R., and Ghoshal, S.P. "Directivity improvement and optimal far

field pattern of time modulated concentric circular antenna array using hybrid evolutionary algorithms", *International Journal of Microwave and Wireless Technologies*, Cambridge University Press, **9**(1), pp.1-14 (June 2015). DOI: http://dx.doi.org/10.1017/S1759078715001075

21. Huang, M., Yang, S., Li, G., and Nie, Z. "Synthesis of low and equal-ripple sidelobe patterns in time-modulated circular antenna arrays", *J. Infrared Milli Terahz Waves*, **30**, pp. 802-812 (2009).
22. Zheng, L., Yang, S., Zhu, Q., and Nie, Z. "Synthesis of pencil-beam patterns with time-modulated concentric circular ring antenna arrays", *PIERS Proceedings*, pp. 372-376, September, Suzhou, China (2011).
23. Mandai, D., Ghoshal, S.P., and Bhattacharjee, A.K., "Design of concentric circular antenna array with central element feeding using particle swarm optimization with constriction factor and inertia weight approach and evolutionary programing technique", *Journal of Infrared Milli Terahz Waves*, **31**(6), pp. 667-680 (2010).
24. Mandai, D., Ghoshal, S.P., and Bhattacharjee, A.K. "Radiation pattern optimization for concentric circular antenna array with central element feeding using craziness based particle swarm optimization", *International Journal of RF and Microwave Computer-Aided Engineering*, **20**(5), pp. 577-586 (September 2010).
25. Ram, G., Mandal, D., Kar, R., and Ghoshal, S.P. "Opposition-based gravitational search algorithm for synthesis circular and concentric circular antenna arrays", *Scientia Iranica, Transactions D, Computer Science & Engineering, Electrical,* **22**(6), p. 2457 (2015).
26. Luo, Z., He, X., Chen, X., et al. "Synthesis of thinned concentric circular antenna arrays using modified TLBO algorithm", *International Journal of Antennas and Propagation* (2015).
27. Singh, U., Salgotra, R., and Rattan, M. "A novel binary spider monkey optimization algorithm for thinning of concentric circular antenna arrays", *IETE Journal of Research*, pp. 1-9 (2016).
28. Das, R. "Concentric ring array", *IEEE Trans. Antennas Propag.*, **14**(3), pp. 398-400 (May 1966).
29. Haupt, R.L. "Optimized element spacing for low sidelobe concentric ring arrays", *IEEE Trans. Antennas Propag.*, **56**(1), pp. 266-268 (January 2008).
30. Stearns, C. and Stewart, A. "An investigation of concentric ring antennas with low sidelobes", *IEEE Trans. Antennas Propag.*, **13**(6), pp. 856-863 (November 1965).
31. Goto, N. and Cheng, D.K. "On the synthesis of concentric-ring arrays", *IEEE Proc.*, **58**(5), pp. 839-840 (May 1970).
32. Huebner, M.D.A. "Design and optimization of small concentric ring arrays", In *ProG. IEEE AP-S Symp.*, pp. 455-45 (1978).
33. Holtrup, M.G., Margulnaud, A., and Citerns, J. "Synthesis of electronically steerable antenna arrays with element on concentric rings with reduced sidelobes", In *Proc. IEEE AP-S Symp.*, pp. 800-803 (2001).
34. Dessouky, M., Sharshar, H., and Albagory, Y. "Efficient sidelobe reduction technique for small-sized concentric circular arrays", *Progress in Electromagnetics Research*, PIER 65, pp. 187-200 (2006).
35. Kaveh, A. and Shokohi, F. "A hybrid optimization algorithm for the optimal design of laterally-supported castellated beams", *Scientia Iranica, Transactions A, Civil Engineering*, **23**(2), p. 508 (2016).
36. Siddique, N. and Adeli, H. "Central force metaheuristic optimisation", *Scientia Iranica, Transactions A, Civil Engineering*, **22**(6) (1941), pp. 1941-1953 (2015).
37. Jolai, F., Reza, T.M., Rabiee, M., et al. "An enhanced invasive weed optimization for makespan minimization in a flexible flowshop scheduling problem", *Scientia Iranica, Transactions E, Industrial Engineering*, **21**(3), p. 1007 (2014).
38. Kaveh, A.A. and Nasrollahi, A. "Charged system search and particle swarm optimization hybridized for optimal design of engineering structures", *Sci. Iran. Trans. A, Civil Eng.*, **21**(2), p. 295 (2014).
39. Hajipour, V., Mehdizadeh, E., and Tavakkoli-Moghaddam, R. "A novel pareto-based multi-objective vibration damping optimization algorithm to solve multi-objective optimization problems", *Scientia Iranica, Transactions E, Industrial Engineering*, **21**(6), p. 2368 (2014).
40. Esmaeili, M., Zakeri, J.A., Kaveh, A., et al. "Designing granular layers for railway tracks using ray optimization algorithm", *Scientia Iranica, Transactions A, Civil Engineering*, **22**(1), p. 47 (2015).
41. Pourbakhshian, S., Ghaemian, M., and Joghataie, A. "Shape optimization of concrete arch dams considering stage construction", *Scientia Iranica. Transactions A, Civil Engineering*, **23**(1), p. 21 (2016).
42. Ram, G., Mandal, D., Kar, R., and Ghoshal, S.P. "Directivity maximization and optimal far-field pattern of time modulated linear antenna arrays using evolutionary algorithms", *AEU-International Journal of Electronics and Communications*, **69**(12), pp. 1800-1809 (2015).

## Biographies

**Gopi Ram** received BE degree in Electronics and Telecommunication Engineering from Government Engineering College, Jagdalpur, Chhattisgarh, India in 2007. He received the MTech degree in "Telecommunication Engineering" from National Institute of Technology, Durgapur, West Bengal, India, in 2011. He joined as a full-time institute research scholar in 2012 at National Institute of Technology, Durgapur, West Bengal, India. His research interests include analysis and synthesis of antenna arrays via evolutionary computing techniques and antenna array optimization of various radiation characteristics. He received the scholarship from the Ministry of Human Resource and Development (MHRD), Government of India in 2007-2009 (MTech) and 2010-2015 (PhD). Currently, he is working as a Senior Assistant Professor at the Department of ECE at Madanpalle Institute of Technology & Science (MITS) (UGC Autonomous). His research interests include antenna array pattern optimization and applications of soft computing techniques in electromagnetic. He has published more than 40 research papers in international journals and conferences.

**Durbadal Mandal** received BE degree in Electronics and Communication Engineering from Regional Engineering College, Durgapur, West Bengal, India in 1996. He received the MTech and PhD degrees from National Institute of Technology, Durgapur, West Bengal, India, in 2008 and 2011, respectively. Presently, he is with National Institute of Technology, Durgapur, West Bengal, India, as an Assistant Professor at the Department of Electronics and Communication Engineering. His research interest includes Array Antenna design and filter optimization via evolutionary computing techniques. He has published more than 230 research papers in international journals and conferences.

**Sakti Prasad Ghoshal** received BSc and BTech degrees in 1973 and 1977, respectively, from Calcutta University, West Bengal, India. He received MTech degree from I.I.T (Kharagpur) in 1979. He received PhD degree from Jadavpur University, Kolkata, West Bengal, India in 1992. Presently, he is acting as a Professor of Electrical Engineering Department of N.I.T. Durgapur, West Bengal, India. His research interest areas are application of evolutionary computing techniques to electrical power systems, digital signal processing, array antenna optimization and VLSI. He has published more than 270 research papers in international journals and conferences.

**Rajib Kar** received BE degree in Electronics and Communication Engineering from Regional Engineering College, Durgapur, West Bengal, India in 2001. He received the MTech and PhD degrees from National Institute of Technology, Durgapur, West Bengal, India in 2008 and 2011, respectively. Presently, he is with National Institute of Technology, Durgapur, West Bengal, India, as an Assistant Professor at the Department of Electronics and Communication Engineering. His research interest includes VLSI signal processing and Filter optimization via evolutionary computing techniques. He has published more than 250 research papers in international journals and conferences.